NESO
National Energy System Operator

Delivered in partnership with

IMPERIAL

WP2 Report

Large-signal System Strength of IBR-dominated Power System

Project: NIA2_NGESO020

NESO
National Energy System Operator

Independent Expert Opinion

Provided by:

Dr. Zitian Qiu, Prof. Tim Green, Dr. Yunjie Gu,

Department of Electrical and Electronic Engineering,

Imperial College London, UK

Disclaimer

This report is the independent expert opinion of the author(s). It does not represent the views of Imperial College London or Imperial Consultants.

Contents

List of Tables

List of Figures

1 Introduction

The power system is transforming from a system dominated by synchronous generators to a system where inverter-based resources (IBRs) become dominant [1]. One consequence is that grid strength is decreasing in some regions in the GB system as thermal power plants with synchronous generators (SGs) are decommissioned in favour of IBRs in the drive to meet the UK's net-zero targets [2].

In conventional power systems that are dominated by SGs, the short-circuit level (SCL), or short-circuit ratio (SCR) is the standard metric of grid strength for evaluating the ability to connect a new device at a specific location. The SCL can be expressed as the SCR, the ratio between the current provided during a three-phase-to-ground fault to the nominal current [3]. Typically, the short-circuit current (SC) contribution (also known as fault current contribution) of an SG can reach 5-7 p.u. [4] because of their low impedance and ability to withstand currents well above normal for short periods without a large and damaging temperature increase. A relatively high SCR results in the generator being seen as a stiff voltage source from the connected point.

However, for an IBR-dominated power system, the system impedances are no longer sufficient to characterise the system [5]. The SC is now tightly regulated by the inverter limits to protect the IGBT, and traditional definitions of SCR are not valid. One of the most common approaches to inheriting the concept of SCR is ignoring the contribution of IBRs. As such, one may be misinformed about the grid strength, e.g., perceiving a low SCR while the system is in fact quite strong. Consequently, the economic viability or maximum power delivery of the connected IBR may not be met.

On the other hand, different control types of IBRs, e.g., grid-forming (GFM) and grid-following (GFL) control, introduce different degrees of effects on the system strength. In practice, a GFM inverter can fix the voltage and angle of the point of interconnection (POI) and is usually considered as a positive role that can increase the system strength [6]. In this case, the GFM inverter should be modelled as a stiff voltage source. While a GFL inverter is typically treated as a current source due to its function of injecting active and reactive power into the grid based on the POI voltage. However, the distinction between GFM and GFL inverters is not well-addressed in the SCR calculation.

To tackle those limitations, we propose a promising metric for evaluating the grid strength based on power flow calculation. We name the proposed metric power margin ratio (PMR).

2 Inadequacy of small-signal metrics for large-signal stability

As we pointed out in the WP1 Report, it is necessary to distinguish between the small-signal and large-signal system strength. In this section, we will conduct electromagnetic transients (EMT) simulations on a single-plant-infinite-bus (SPIB) system to elaborate the reason.

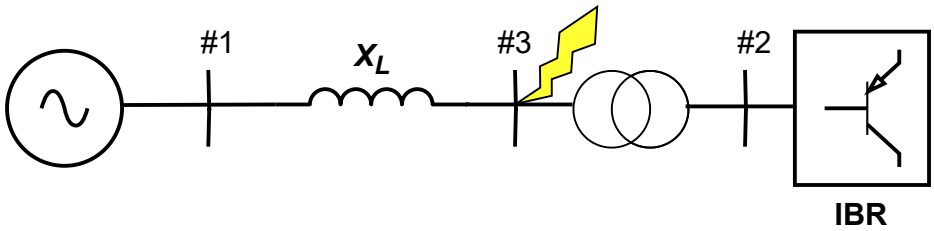

Fig. 1: Single line diagram of the SPIB system

Consider the SPIB system shown in Fig. 1, where all physical quantities are in per unit. Let the line impedance $X_L = 1/1.12$ with resistance ignored, and the nominal power of the IBR $P_{IBR,nom} = 1$. In this case, we assume that the IBR is also injecting 1 p.u. active power into the grid. The IBR is a GFL inverter with PV control. A three-phase short circuit is triggered at Bus #3 at 50 s and lasts for 4 cycles. We set high fault resistance to model the system perturbed by small disturbances and small fault resistance for large disturbances.

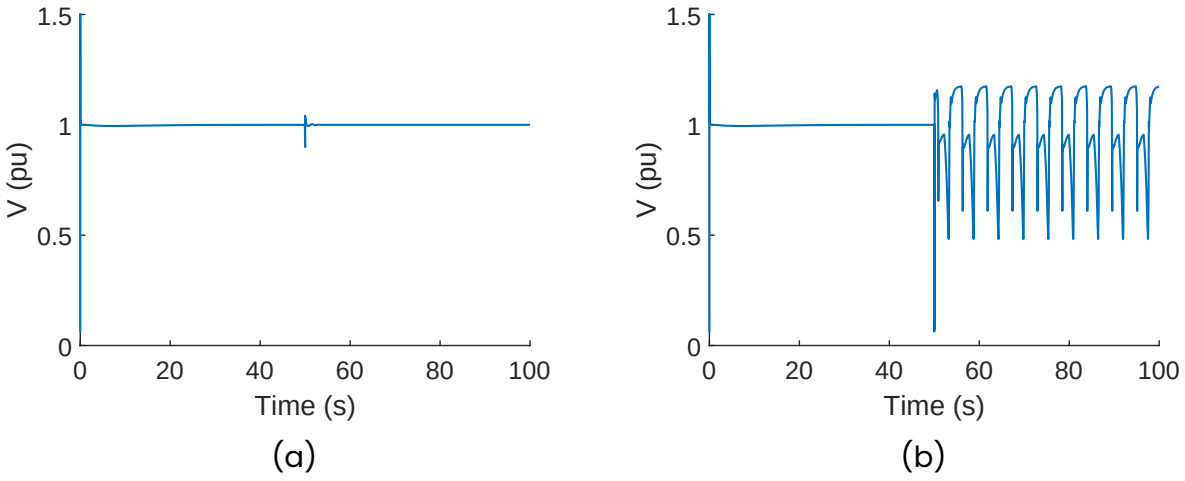

Fig. 2: Voltage at Bus #3 based on EMT simulations of the SPIB system under (a) small disturbance and (b) large disturbance.

The EMT simulation results are presented in Fig. 2. It is clear in Fig. 2 (a) that when the system suffers a small disturbance, the voltage drops to 0.9 p.u. The voltage of the IBR bus can recover after the fault, implying that the system is stable in the small signal sense. On the contrary, when the voltage drops heavily during the fault, the voltage of the IBR bus cannot recover after the fault is cleared, which is shown in Fig. 2 (b). It leads to large-signal instability of the system. Moreover, the large-signal instability does not exhibit oscillations with increasing amplitude, which is different from the typical small-signal instability mechanism. Hence, we can conclude that such instability is not a small-signal problem. As a result, it is inadequate to use small-signal metrics for large-signal stability assessment.

3 Power margin ratio

This section starts by briefly reviewing the calculation of the SCR, followed by a detailed discussion of the proposed PMR. Our understanding and comments on PMR are summarized at the end as the takeaways of this section.

3.1 Short-circuit ratio (SCR)

Since SCR has been widely used for system strength assessment of SG-dominated power systems, it is important to review its concept and understand the principle.

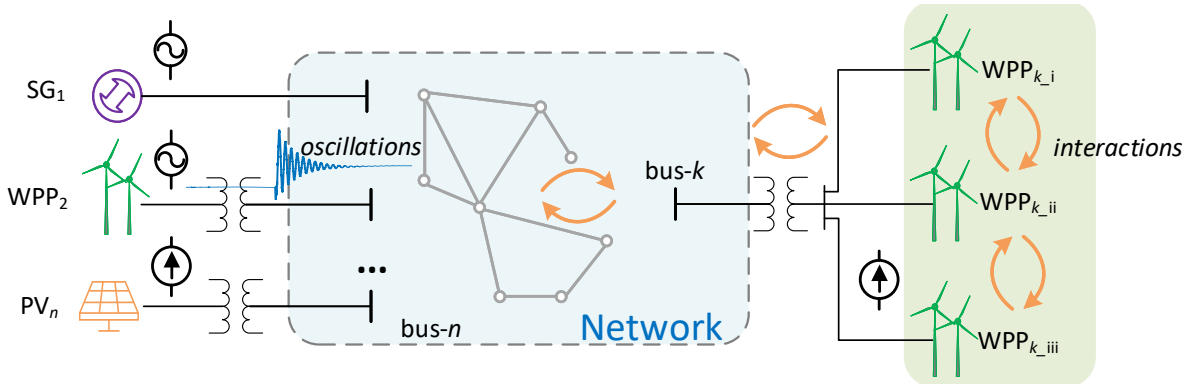

Fig. 3: A typical structure of an IBR-dominated power system

Fig. 3 presents a typical structure and components of an IBR-dominated power system, where wind power plants (WPPs) and photovoltaic (PV) plants are inverter-interfaced power generation units. Regardless of the generation-side control to achieve power converting, we focus on the interaction of the grid-side converter with the grid. When viewed from a single bus, e.g., bus-k, a model equivalence can be made on the rest of the system to create an equivalent ideal voltage source in series with a Thevenin impedance, as shown in Fig. 4. V_s is the equivalent Thevenin voltage; $Z_{th,k}$ is the Thevenin impedance seen from bus-k; and $I_{s,k}$ is the current flow from the source V_s.

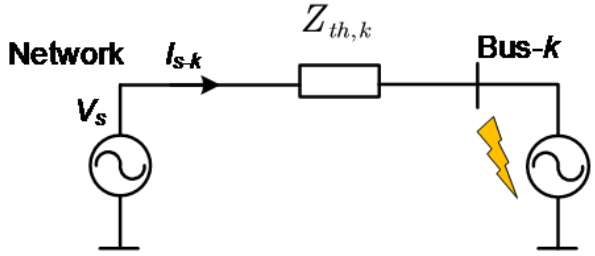

Fig. 4: Circuit representation of a plant connected to an infinite bus

When a three-phase-to-ground short-circuit happens at bus-k, i.e., bus-k is connected to the ground through small impedance, the power flows from the system to bus-k is defined as the short-circuit capacity (SCC), or short-circuit level (SCL) at bus-k, and is expressed as

$$SCC_k = \frac{|V_s|^2}{|Z_{th,k}|}. \tag{1}$$

SCR is then defined as the ratio between SCC_k and the nominal power $P_{k,nom}$ of the device connected to bus-k, i.e.,

$$SCR_k = \frac{SCC_k}{P_{k,nom}}. \tag{2}$$

If all the physical quantities in Fig. 4 are in per unit where the voltage $V_s = 1$ p.u., SCR can be expressed in the following equation:

$$SCR_k = \frac{1}{|Z_{th,k,pu}|P_{k,nom,pu}}. \tag{3}$$

Since in the following sections of this Report, all the discussion is put in the per unit system, we discard the subscripts of pu and nom for simplicity.

In a conventional power system where only SG exists, the SCR defined based on short-circuit capacity is completely consistent with the SCR defined by the Thevenin equivalent impedance, since the short-circuit current of the synchronous generator is entirely determined by its impedance, without any current limiters [7]. However, due to the overcurrent limiters of the IBRs, the short-circuit capacity is no longer a quasi-linear output characteristic. Therefore, the SCR based on the short-circuit capacity definition and the SCR based on the Thevenin equivalent impedance definition are fundamentally different for the IBRs. As revealed in Section 2, there exists drastic differences between small- and large-signal dynamics of the IBR-to-grid system. To address the limitations of SCR-based metrics for (large-signal) grid strength evaluation of IBR-dominated systems, we propose an alternative indicator named *Power Margin Ratio*.

3.2 Power margin ratio (PMR)

The basic idea behind using the PMR to assess the system's strength is to determine the maximum power a bus can handle while still maintaining a static operating point. Compared to the SC current calculation which requires the "source + impedance" combination of the plant, power itself is a more intuitive and direct information for grid strength evaluation since it can be obtained by power flow calculation.

Given a power system as shown in Fig. 3, the PMR of bus-k is calculated as

$$PMR_k = \frac{P_{k,max}}{P_{IBR}}, \tag{4}$$

where $P_{k,max}$ is the maximum power the system can absorb from this POI and P_{IBR} is the nominal power of the connected IBR. $P_{k,max}$ can be acquired from power flow calculation by increasing the output power at the corresponding POI until reaching a non-converged result.

When conducting power flow calculations, we specify the node types for different generation plants as in Table 1. It should be noted that in steady state power flow calculation, the GFM can be treated as a PV bus. However, in PMR calculation, the power flow refers to the one within a short transient period. As a result, the GFM is assumed to be a stiff Vθ node, where the power angle aligns with the pre-fault value.

Table 1: Node types adopted in PMR calculation

Plant type	Node type
GFL with PQ control	PQ
GFL with PV control	PV
GFM	Vθ
Infinite bus	Slack

Similar to the SCR, a larger PMR implies a stronger grid, i.e., the system is more likely to operate in a stable manner and for the system as a whole to recover intact from major disturbances [8].

3.3 Relation between PMR and SCR

For the SPIB system shown in Fig. 1, the PMR is identical to the conventional SCR. The reason is that the POI is the only point where an IBR can be integrated. The interaction can only take place between the IBR and the infinite bus, where the infinite bus is a stiff voltage source with constant voltage magnitude and frequency. Hence, the Thevenin impedance X_L entirely captures the grid strength in the per-unit system, as given in Eqn. (3). On the other hand, the active power that can be transferred between the IBR and the infinite bus is

$$P = \frac{V_s V_i}{X_L} \sin(\Delta\delta), \tag{5}$$

where V_s and V_i are voltages of the infinite bus and IBR; $\Delta\delta$ is the angular difference between two nodes. Therefore, the maximum power delivered is $P_{\text{max}} = 1/X_L$ in p.u. Substituting P_{max} into Eqn. (4) and comparing it with Eqn. (3) shows that PMR and

SCR are identical for the SPIB system.

However, it becomes different in multi-IBR systems. In general, the contributions of IBRs to the grid strength are ignored when calculating the SCR of IBR-dominated power systems. From the power flow viewpoint, the IBRs are assumed to inject zero power into the grid, while the PMR involves the actual and potential power output with respect to the type of IBRs. Case studies are reported in Section 4.2.1 and Section 4.2.2.

3.4 Discussions of the PMR

PMR provides a technology-neutral definition of system strength that is naturally suitable for multi-infeed, large-signal system analysis and is simple to calculate. Moreover, GFL with PQ control, GFL with PV control, and GFM inverters are classified as different nodes in power flow calculation, leading to a type-dependent large-signal system strength metric. As such, for instance, one can clearly reveal the benefit of integrating GFM inverters to improve the grid strength. Precisely, a larger PMR can be obtained if a GFL inverter is replaced by a GFM inverter. Since PMR requires power flow calculation, the interaction among different buses is naturally involved. It is worth noting that to calculate the PMR, one may have to modify the conventional power flow algorithm to include multiple $V\theta$ buses in the case where GFM inverters exist.

The PMR is defined with the nominal power of the IBR in Eqn. (4). This is actually the "worst case" definition of the system strength. For a specific operating scenario, it is fair to calculate the PMR with the IBR's actual output power.

PMR cannot reveal exactly how the transient power flows, and it is not a rigorous certificate for the transient stability of power systems. It cannot assert whether the system is stable or not after a disturbance. In fact, fault recovery is closely regulated by the control implementation and interactions of different control loops, which are discussed in detail in Section 4.

4 EMT Simulation results

All EMT simulations reported in this section are conducted in MATLAB/Simulink.

4.1 Single-plant-infinite-bus system

First, we adopt the SPIB system as a demonstration of the PMR. The system is given in Fig. 1. The nominal power of the IBR is fixed at 1 p.u., while the line's static power transfer limit (in terms of the line's impedance) is varied. The equivalent impedance of the transformer is 0.05 p.u.

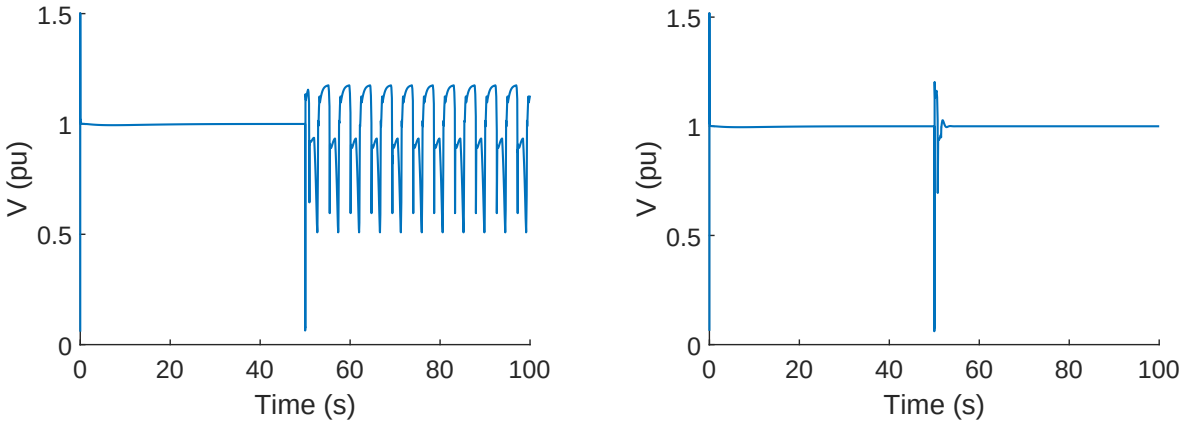

Fig. 5: Voltage of the IBR based on EMT simulations of the SPIB system under (a) $X_L = 1/1.1$ and (b) $X_L = 1/1.2$.

The voltages of the IBR under different line impedances based on EMT simulation results are presented in Fig. 5. In the first setting where $X_L = 1/1.1$, it can be seen that the system can stably operate before the fault occurs, but fails to recover after the fault is cleared. In the second setting where $X_L = 1/1.2$, the system can withstand the fault. The calculated PMRs for both cases are $PMR_{X1} = 1.043$ and $PMR_{X2} = 1.132$, respectively. Therefore, two conclusions can be drawn from the EMT simulation. 1) Similar to the SCR, a larger PMR implies a stronger grid, i.e., the system is more likely to operate in a stable manner and for the system as a whole to recover intact from major disturbances. 2) The PMR is not a rigorous certificate for stability assessment of power systems. That is, although $P_{IBR} = 1 < 1.043$, the system still fails to recover from a fault. In fact, the fault recovery process is largely dependent on the IBR's detailed control implementation, which is beyond the ability of the PMR.

Next, we fix the line's static power transfer limit at $X_L = 1/1.13$ and vary the nom-

inal power of the IBR. To align with the definition of PMR, we let the IBR actually output its nominal power. The voltages of the IBR based on EMT simulation results are presented in Fig. 6. When the nominal power of IBR is 1.05, the system cannot recover from the fault, while reducing P_{IBR} to 1 p.u. can make the system withstand the fault. The calculated PMR for both case are $PMR_{P1} = 1.019$ and $PMR_{P2} = 1.070$, respectively. This comparison confirms that a higher PMR value implies a stronger grid. Moreover, PMR can reveal the impact of the output/nominal power of the IBR on the system strength.

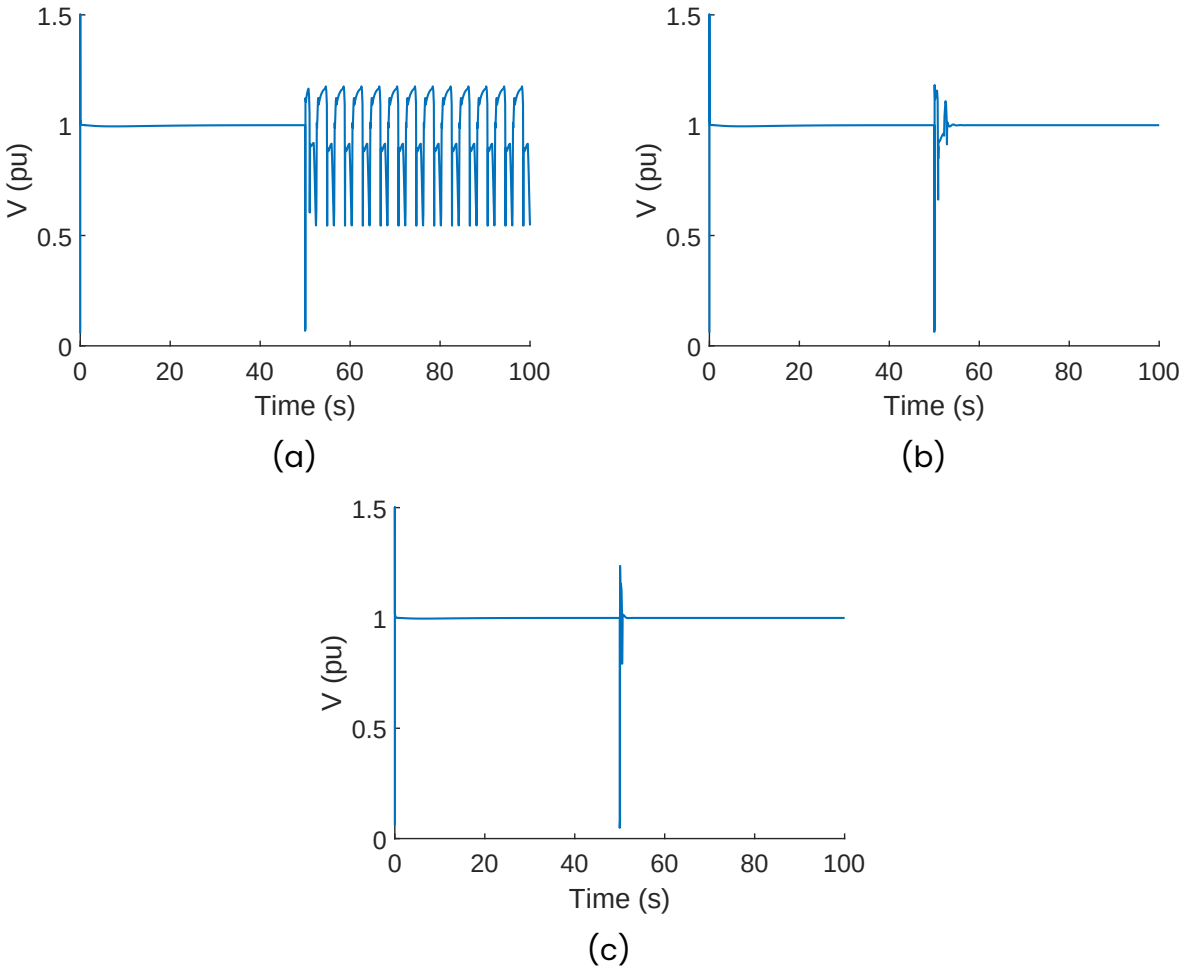

Fig. 6: Voltage of the IBR based on EMT simulations of the SPIB system under (a) $P_{IBR} = 1.05$, (b) $P_{IBR} = 1$, and (c) $P_{IBR} = 1$ while the actual output power $P_I = 0.8$.

Furthermore, we can regard $PMR_c = 1.070$ as the critical PMR for this fixed-topology system with adjustable IBR output power. Then, any PMR greater than PMR_c ensures that the system can withstand the same short-circuit fault. Generally, given a fixed line impedance, $PMR > PMR_c$ may appear in the IBR with either a smaller nominal power or a reasonable nominal power but with a smaller actual output power. The

former can be directly deduced from Eqn. (4), and the latter can be obtained by using the actual output power of the IBR as the denominator in Eqn. (4). Fig. 6 (c) illustrates the voltage of IBR in a scenario where the nominal power is $P_{IBR} = 1$ while the actual output power is $P_I = 0.8$. It is evident that the system can withstand the fault. Since the actual power of IBR is smaller than 1 p.u., the PMR becomes larger than PMR_c. As a result, reducing the normal operating output power of an IBR can improve system strength if no interactions with other IBRs.

4.2 Two-IBR-infinite-bus system

We now consider a two-IBR-infinite-bus system which the single-line diagram and bus numbering of which are shown in Fig. 7. For simplicity, we denote this system as the two-IBR system. All the faults triggered in this section are three-phase-to-ground short-circuit faults with low fault impedances.

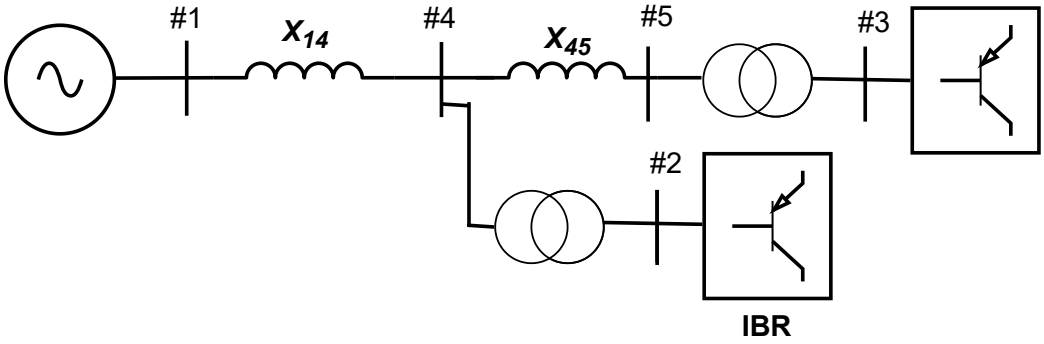

Fig. 7: Single-line diagram and bus numbering of the two-IBR-infinite-bus system.

In Section 4.2.1 and 4.2.2, we use EMT simulations to demonstrate that the SCR is not a proper metric for grid strength evaluation of IBR-dominated power systems, while the PMR can fulfil this role. We study the type-dependent feature of the PMR and show how PMR can reveal the benefit a GFM inverter can bring to the system compared to a GFL inverter in Section 4.2.3. Finally, the relation of PMR, transient stability, and transient power flow is discussed in Section 4.2.4.

4.2.1 High SCR while the system is prone to unstable

We first examine the strength of Bus #4 (which is electrically equivalent to Bus #2 due to the negligible impedance of the transformer). The lines' power transfer limits are $X_{14} = 1/4$ and $X_{45} = 1/1.3$ in per unit, respectively. Both IBRs generate 1 p.u. active power. The fault is applied near Bus #4. Both IBRs are GFL inverters with PV control.

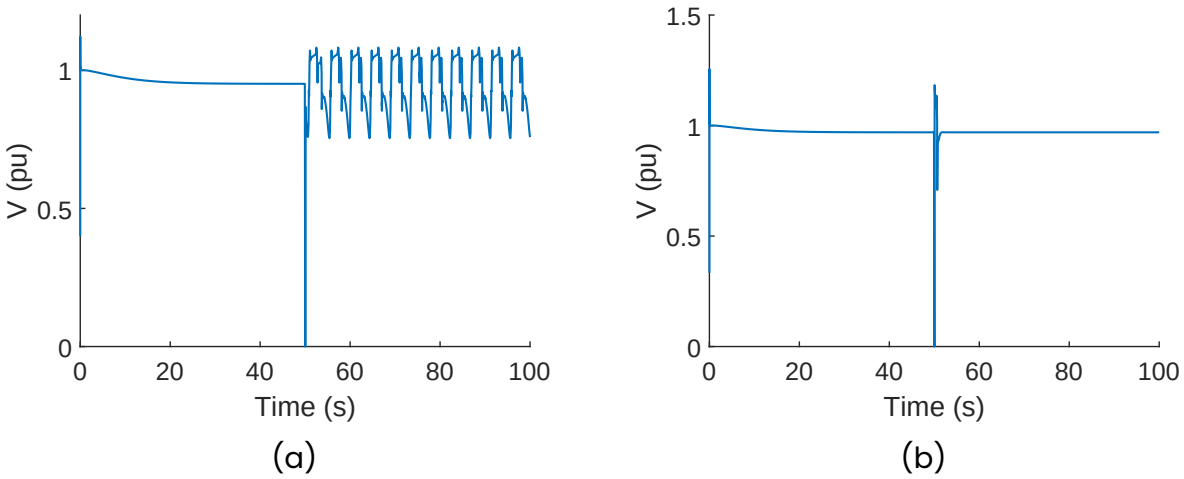

Fig. 8: Voltage at Bus #4 based on EMT simulations of the two-IBR system (a) without IBR aggregation and (b) with IBR aggregation.

The voltage at Bus #4 is presented in Fig. 8 (a). As shown, the system can stably operate at a steady state while it cannot recover from a fault. The SCR at Bus #4 is 4 based on the definition of Eqn. (3), which is considered relatively high. However, the system exhibits oscillatory behavior following the fault. Therefore, ignoring the contribution of IBRs can lead to an inaccurate assessment of the system strength.

Moreover, it should be noted that aggregating the IBRs by simply adding their nominal powers is not a valid solution. At pre-fault steady state, the power transferred from Bus #4 is 2 p.u. and 1 p.u. from Bus #3, implying that both lines can accommodate such amount of power delivered in a static sense. On the other hand, when we aggregate all IBRs that are located downstream of Bus #4 so that the equivalent IBR has a nominal power of 2 p.u., the two-IBR system is transformed into an SPIB system. The EMT simulation results of the equivalent system are shown in Fig. 8 (b). This system can withstand the fault and successfully return to stable operation. The reason is that the strength of Bus #4 is not merely determined by line X_{14}, its downstream line X_{45} plays a crucial role in evaluating the strength of the bus. Ignoring the constraints imposed by other connected lines nearby may lead to an incomplete view of the bus's strength.

4.2.2 Low SCR while the system is strong

We then study the strength of Bus #3 (or Bus #5 since the equivalent impedance of the transformer is quite small). The lines' power transfer limits are $X_{14} = 1/4$ and $X_{45} = 1/1.4$ in per unit, respectively. Both IBRs generate 1 p.u. of active power. The fault is applied near Bus #5.

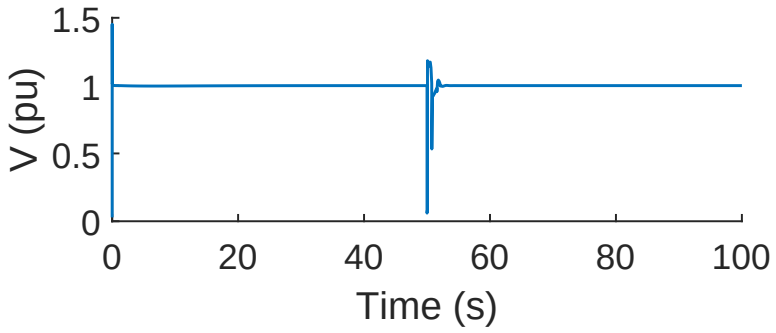

Fig. 9: Voltage at Bus #3 based on EMT simulations of the two-IBR system

The voltage profile at Bus #3 is presented in Fig. 9, where the system is stable after the fault is cleared. Both IBRs are GFL inverters with PV control. Based on the definition in Eqn. (3), the SCR of Bus #3 is 1.037. It is close to 1, approaching the system's stable operating boundary. Such a low SCR typically implies a high likelihood of instability when the system experiences a disturbance. However, from Fig. 9, the system can withstand even a severe three-phase-to-ground fault. To this end, the SCR is no longer a reliable metric to evaluate the system strength in such scenarios. The system may be strong enough to withstand a severe fault when the SCR is low.

Now we illustrate that the PMR is a better metric for system strength evaluation. By setting Bus #2 and #3 as PV buses, and Bus #4 and #5 as PQ buses with zero active and reactive power, we conduct power flow calculations by gradually increasing the active power injection at Bus #3. The maximum power for Bus #3 such that the power flow has a converged result is 1.2. Hence, the PMR of this bus is $PMR_3 = 1.2$. Compared with the conventional SCR, the contribution of IBR at Bus #2 is involved in the PMR. Precisely, the PMR captures the voltage support function of the IBR at Bus #2 for which a direct AC voltage control is applied.

4.2.3 Studies on the type-dependency of the PMR

The PMR is a type-dependent metric that can distinguish different control modes of the IBR, i.e., GFM and GFL with PQ/PV control (GFL_PQ/GFL_PV).

Following the case in Section 4.2.2, the power flow at steady state is listed in Table 2 where IBR #2 is a GFL_PV. To make a comprehensive illustration of the type-dependent feature of the PMR, we fix the system topology and make different combinations in the control mode of those two IBRs. We consider 6 different combinations of IBRs, i.e., IBR #2 takes from GFM, GFL_PQ, and GF_PV, while IBR #3 is chosen either GFL_PQ or GFL_PV. We evaluate the strength of Bus #3 under each configuration.

We find that using the line impedance $[1/4, 1/1.4]$ in PMR calculation leads to close

Table 2: Power flow of the two-IBR system in Fig. 7 where $X_{14} = 1/4$, $X_{45} = 1/1.4$

Bus number	V_{amp} (p.u.)	δ (°)	P (p.u.)	Q (p.u.)
1	1	0	-2	0.75
2	1	34.45	1	0.92
3	1	84.73	1	0.56
4	0.95	31.54	0	0
5	0.97	81.83	0	0

results for GFM and GFL_PV since power transfer through line X_{45} is restricted by its large impedance. Hence, for better illustration, we modify the line impedance as $[1/3, 1/2]$. The power flow at steady state is listed in Table 3 where IBR #3 is a GFL_PV.

Table 3: Power flow of the two-IBR system in Fig. 7 where $X_{14} = 1/3$, $X_{45} = 1/2$

Bus number	V_{amp} (p.u.)	δ (°)	P (p.u.)	Q (p.u.)
1	1	0	-2	0.97
2	1	47.38	1	1.00
3	1	79.82	1	0.41
4	0.95	44.46	0	0
5	0.98	76.93	0	0

The calculated PMR values of Bus #3 is listed in Table 4. When Bus #3 is a PQ bus, we assume that the reactive current reference is identical to the one in Table 2. Among all configurations, the combination of GFM+GFL_PV yields the highest PMR, while the lowest PMR appears when both IBRs are GFL_PQs. Moreover, comparisons among GFL combinations illustrate that AC voltage control leads to a larger PMR. For this case, voltage control applied to the upstream bus benefits the system. This coincides with the intuition that applying voltage control helps bus voltage become "stiffer" and improves grid strength.

Table 4: PMR of BUs #3 of the two-IBR system with different combinations of IBRs

Bus #2	Bus #3	PMR
GFL_PV	GFL_PV	1.50
GFL_PQ	GFL_PV	1.06
GFM	GFL_PV	1.62
GFL_PV	GFL_PQ	1.07
GFL_PQ	GFL_PQ	1.00
GFM	GFL_PQ	1.09

If we apply PQ control to Bus #2 where the reactive power reference is identical to the power flow result, the IBR voltage cannot recover to its nominal value after the fault is cleared, as shown in Fig. 10 (a) – (f). When the voltage rises after the fault, the reactive power is still below the set value, resulting in an increase in i_q^{ref}. Moreover,

the dynamic of i_d, for example, is regulated by:

$$L\frac{\mathrm{d}i_d}{\mathrm{d}t} = v_{cd} - v_d - \omega L i_q, \tag{6}$$

where v_{cd} is the converter's d-axis voltage and v_d is the d-axis of the point of coupling (PCC); ω is the angular frequency of the PLL. Due to the voltage amplitude of the converter being limited to a maximum of 1.2 p.u., the change rate of i_d is negative most of the time (see 10 (d)). The integral of the positive segments over time cannot compensate for that of the negative intervals. The current cannot "pull back" to track the reference value. As a result, the current controller fails (see Fig. 10 (a)), leading to the voltage losing control. Reducing the power output of IBR #3 to 0.9 p.u. can make the system successfully recover from the fault. From the system perspective, GFL with PQ control lacks the capability for direct voltage control. Hence, based on the concept of grid strength, the bus connecting a GFL_PQ is relatively "weaker" than that of a GFL_PV.

A prominent benefit of the PMR lies in the ability to reveal the difference between GFL_PQ and GFL_PV. Compared with GFL_PV mode whose PMR is 1.2, the PMR for GFL_PQ is reduced to 1.05. Given the same structure of the grid, the reduction in the PMR implies that the GFL_PQ is more likely to lose stability after the system is severely disturbed.

We also verify the stability by conducting EMT simulations, and the voltage at Bus #3 is presented in Fig. 11. We omit the voltage profile of Bus #2 since it shows similar results. The power output of the IBR #3 is set to 1.05 p.u. In GFL_PV mode, the system oscillates after the fault is cleared. On the contrary, connecting a GFM at Bus #2 facilitates the recovery of the system after a fault. The GFM behaves like a stiff voltage source which provides strong voltage support to the grid. Comparing the first three rows of Table 4, the PMR for the GFM case is the largest, which is in line with the EMT simulation results. *In conclusion, in terms of grid support, GFM>GFL_PV>GFL_PQ.*

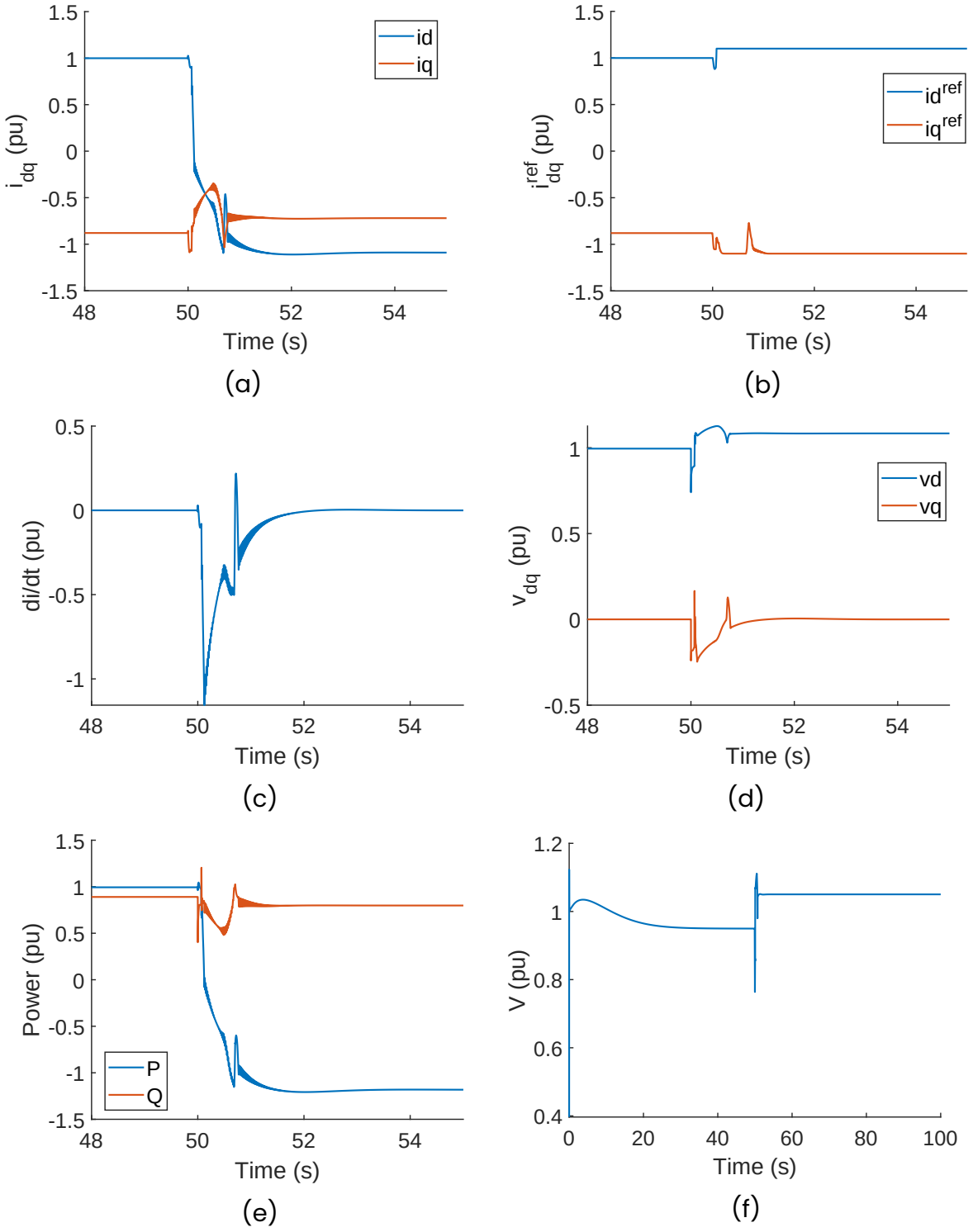

Fig. 10: Voltage and current of $d-$ and $q-$ axis as well as active/reactive power of the IBR #2. (a) measured current i_{dq}; (b) current reference i^{ref}_{dq}; (c) rate of change of d-axis current $\frac{\mathrm{d}i_d}{\mathrm{d}t}$; (d) PCC voltage in d- and q-axis v_{dq}; (e) active and reactive powerPQ; and (f) PCC Voltage V.

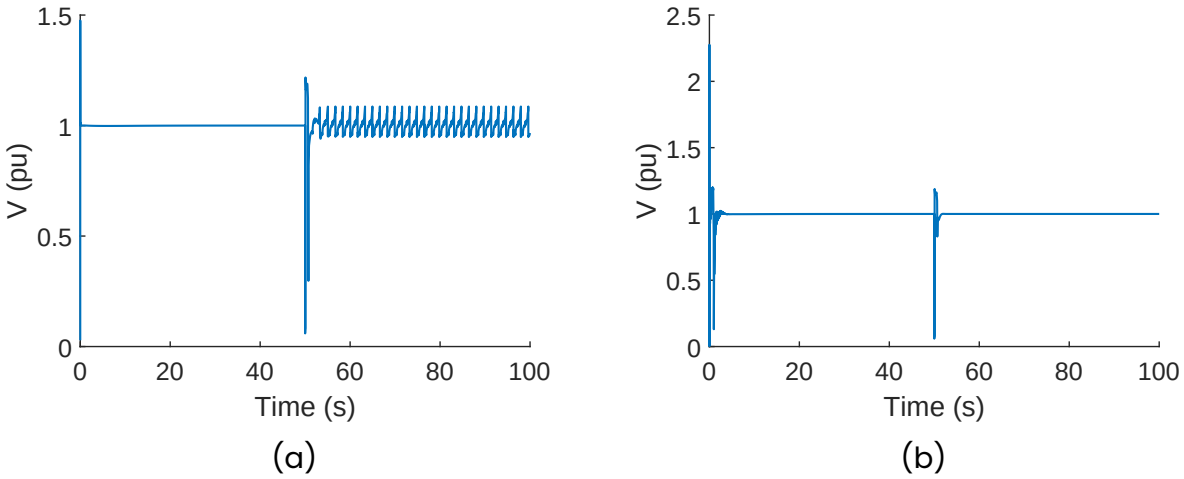

Fig. 11: Voltage at Bus #3 based on EMT simulations of the two-IBR system (a) GFL_PV and (b) GFM.

The calculated PMR values of Bus #2 is listed in Table 5. When Bus #2 is a PQ bus, we assume that the reactive current reference is identical to the one in Table 3. Among all configurations, the combination of GFM+GFL_PV yields the largest PMR while the smallest PMR appears when both IBRs are GFL_PQs. Similarly, the bus with voltage support has higher strength than that without voltage controls. GFM inverters can significantly enhance the system strength.

Table 5: PMR of BUs #2 of the two-IBR system with different combinations of IBRs

Bus #2	Bus #3	PMR
GFL_PV	GFL_PV	1.61
GFL_PV	GFL_PQ	1.46
GFL_PV	GFM	3.00
GFL_PQ	GFL_PV	1.10
GFL_PQ	GFL_PQ	1.00
GFL_PQ	GFM	1.81

4.2.4 Discussion of PMR, transient power flow, and transient stability

We now point out that the PMR and transient stability are related but not closely coupled. That is, the instability is mainly due to the interaction of the control loops of the IBR. To show this, we consider the two-IBR system with line impedances $X_{14} = 1/3$ and $X_{45} = 1/2$. The nominal power of IBR #3 is set to 1.05 p.u. As shown in Fig. 11 (a), the system cannot recover to its normal operation after clearing the fault. Following the EMT simulations, we present the active and reactive power profiles in Fig. 12. Nevertheless, if we reduce the integral gain of the PI controller of the AC voltage control,

the system can recover from a fault. The EMT simulation results are illustrated in Fig. 13. (Alternatively, reducing the bandwidth of the PLL can also bring the system back to normal operation.)

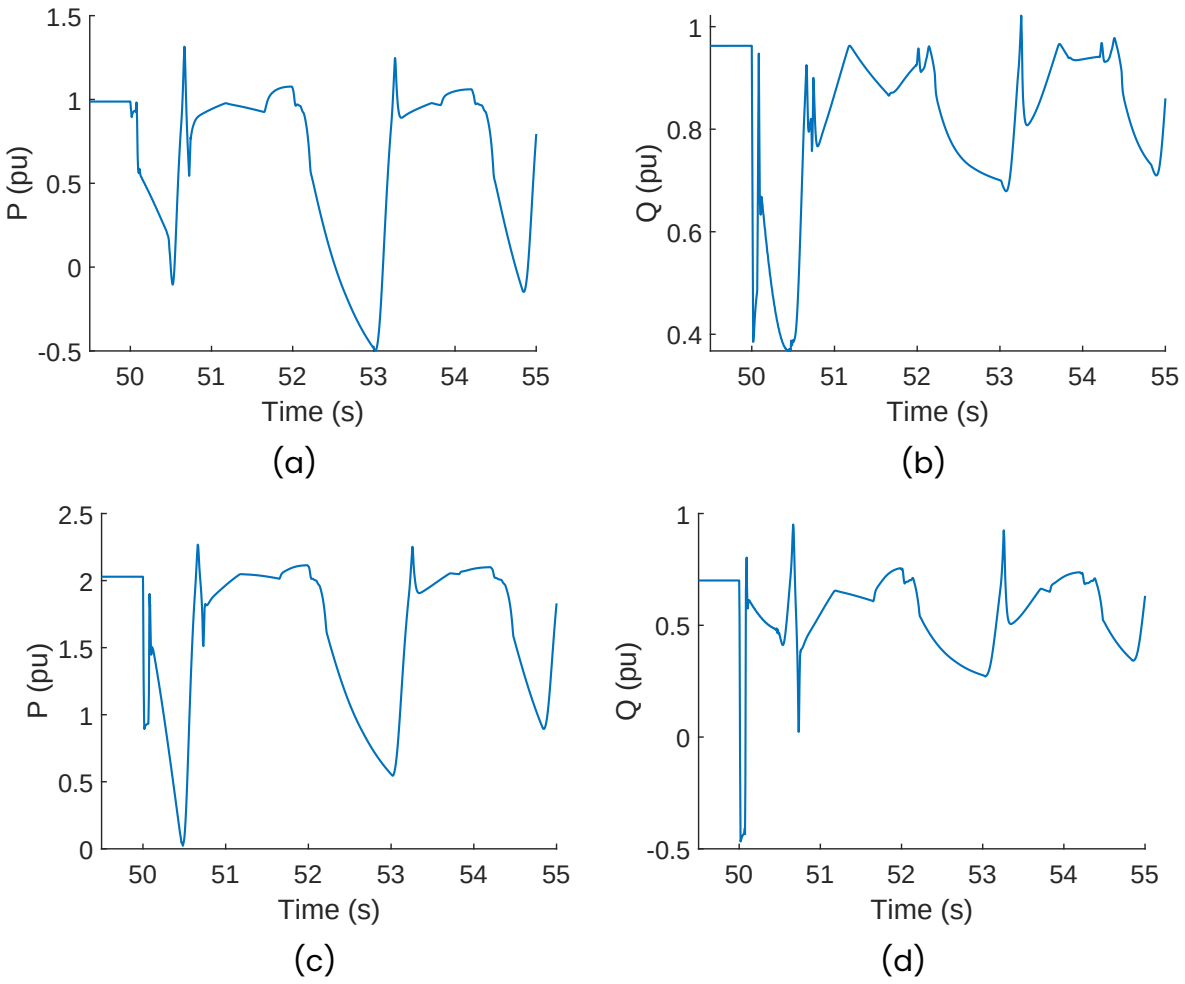

Fig. 12: Unstable case: active/reactive power of the GFL IBR #2 and the power transferred to grid through X_{14} during the transient period. (a) P of the GFL; (b) Q of the GFL; (c) P flow from Bus #2 to the grid; (d) Q flow from Bus #2 to the grid.

Comparing Fig. 13 (a) – (b) Fig. 12 (a) – (b), GFLs with different control parameters have almost the same transient behaviour in terms of active and reactive power during the fault-on period (starts from $t = 50$ s and lasts 4 cycles). However, the stability divergence occurs at $t = 52$ s. This indicates that the plant's transient power flow during fault is not the main cause of the instability. On the other hand, the power flow on lines are quite similar to each other for those two cases before $t = 54$ s. As a result, the line power flow offers limited insight into the stability of the system. Based on the above discussion, the instability of the system is a control-related problem that can not be fully reflected by the transient power flow or the PMR.

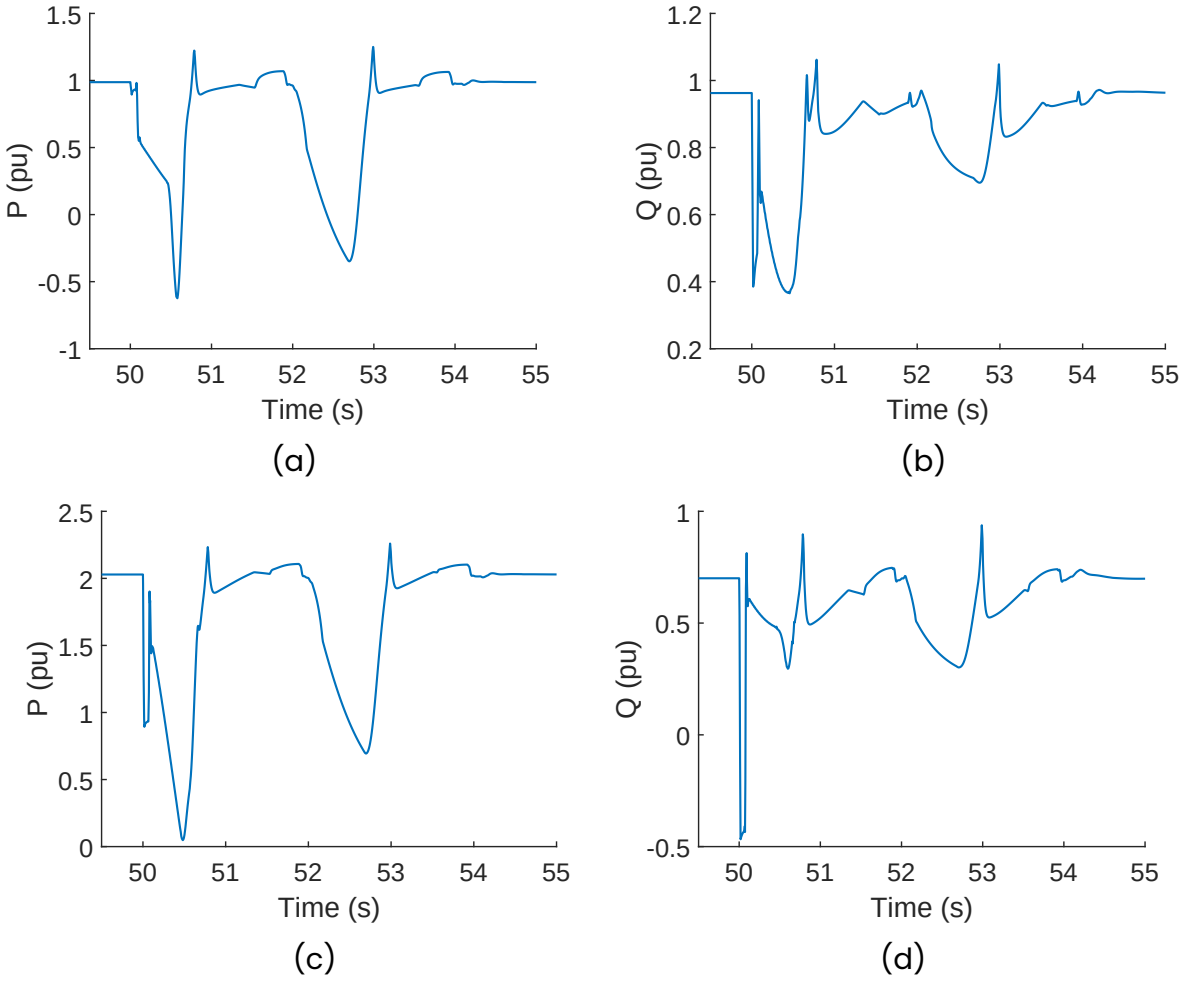

Fig. 13: Stable case: active/reactive power of the GFL IBR #2 and the power transferred to grid through x_{14} during the transient period. (a) P of the GFL; (b) Q of the GFL; (c) P flow from Bus #2 to the grid; (d) Q flow from Bus #2 to the grid.

On the other hand, transient power flow can partially reflect the transient stability of the system. During the fault, a GFM inverter behaves differently from the GFL inverter. The active and reactive power of the IBR and transferred through line X_{14} are plotted in Fig. 14 where the nominal power of IBR #3 is 1.05 p.u. Comparing Fig. 14 to Fig. 12 and Fig. 13, GFM inverters can inject additional active and reactive power during the fault. This is in line with the assumption that a GFM functions as a Vθ bus where the power follows the entire demand of the grid. Qualitatively, the GFM inverter has strong voltage support, leading to less voltage and angle deviation of Bus #4, as is presented in Fig. 15. Due to this, more power can be transferred from Bus #4.

In PMR calculation, we tend to use static information to reveal the transient behaviour of the system. For instance, we assume the GFM inverter is a Vθ bus, although the angle of the GFM is actually not constant during the transient period; GFL_PV is

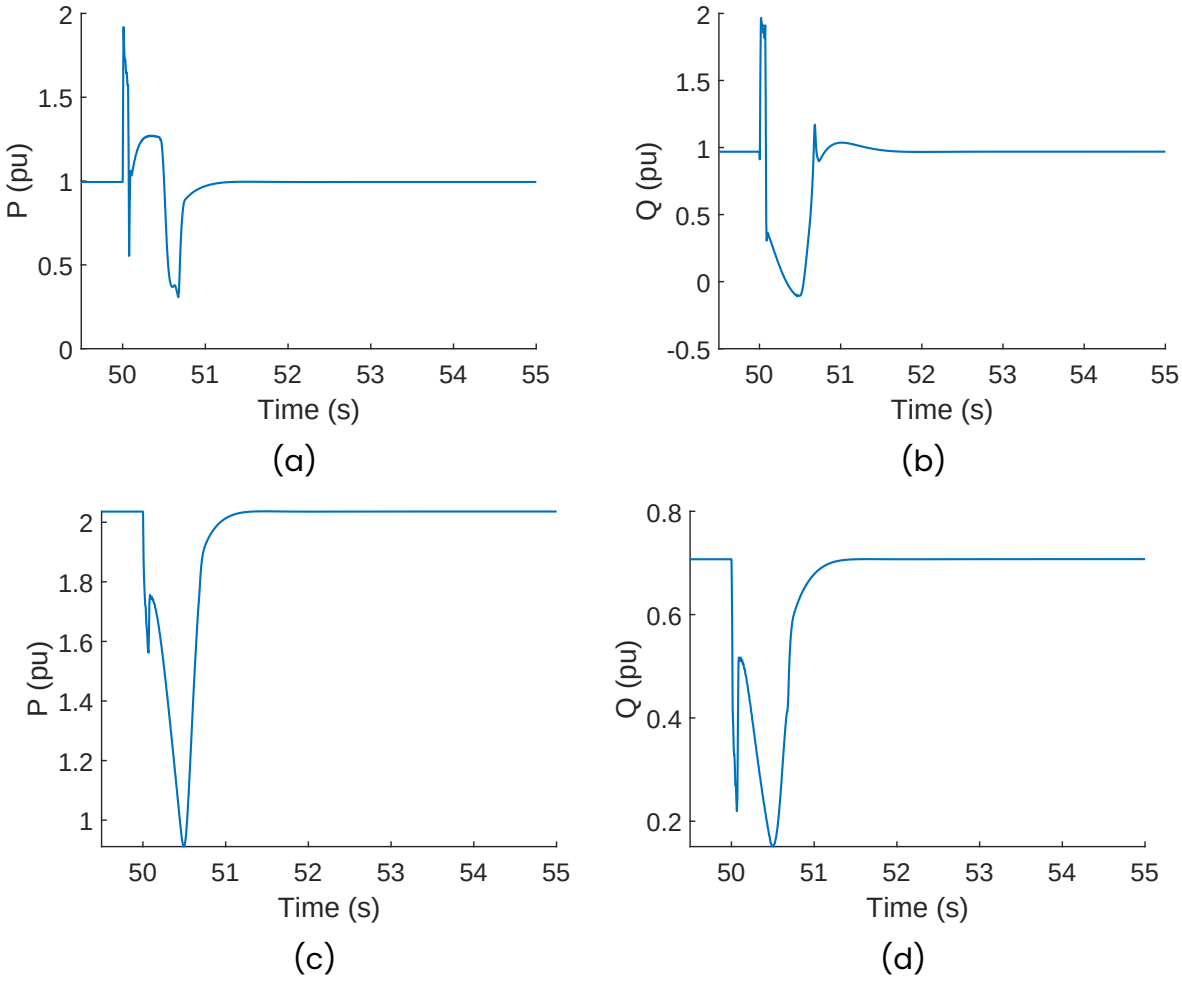

Fig. 14: Active/reactive power of the GFM IBR #2 and the power transferred to grid through x_{14} during the transient period. (a) P of the GFM; (b) Q of the GFM; (c) P flow from Bus #2 to the grid; (d) Q flow from Bus #2 to the grid.

assumed as a PV bus, whereas the voltage is not constant during the transient period. These assumptions make the PMR not a rigorous characterization of the stability of the power system. PMR may lead to an optimistic evaluation of the grid's stability. However, the PMR captures the key features of distinct control modes of IBRs. Exploiting such features, the degree of contribution to the grid strength from different types of IBRs is involved.

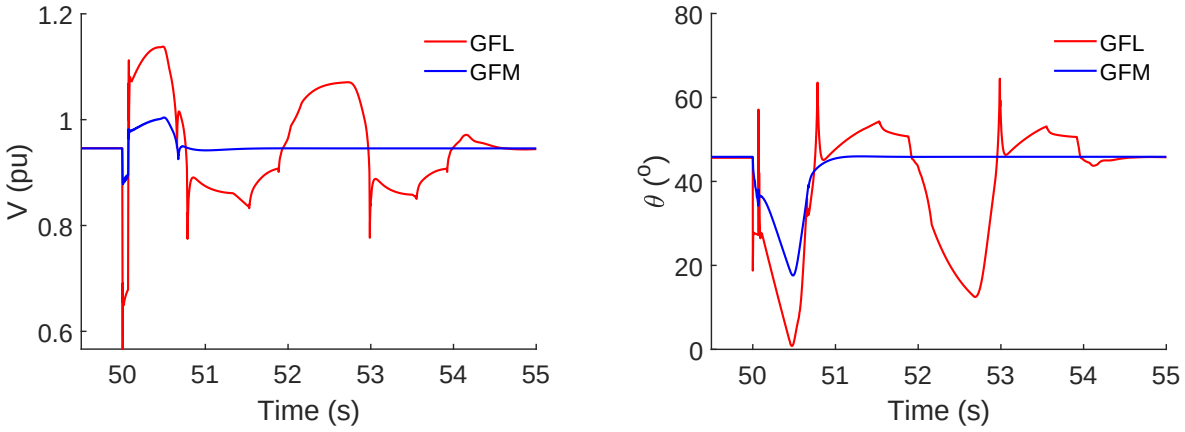

Fig. 15: Voltage and angle of Bus #4 based on EMT simulations of the two-IBR system (a) GFL_PV and (b) GFM.

4.3 Source-load coexisting power systems

Since the PMR is a power flow-based metric for large-signal system strength evaluation, it can be naturally extended to the source-load coexisting power systems. To show this, we consider a SPIB system with a constant power load (CPL) as shown in Fig. 16. The CPL is connected in parallel at the same POI as the IBR. Typically, CPLs include power electronics interfaced loads, such as computers, televisions, etc, to variable speed drive interfaced motor loads [9]. Besides consuming constant power over a user-specified voltage range, CPLs exhibit a linear reduction in the power consumption as the voltage drops below the user-specified voltage range, to represent the undervoltage trip of these devices. In our simulation, to model the CPL, we adopt the same structure of the IBR, while the power reference is a negative value, and no terminal AC voltage is adopted. Moreover, if the voltage drops below 0.5 p.u., the CPL switches to power reduction mode. The line impedance is set to $X_L = 1/1.5$ p.u. The IBR is a GFL inverter with PV control.

By conducting EMT simulations, the stable and unstable cases under the same severe three-phase-to-ground faults are illustrated in Fig. 17. The blue cases imply the system can recover from the fault under such IBR-CPL output level, while the red ones fails. From the results, we can draw the following conclusions:

- This IBR-CPL case illustrates that the system strength can be viewed from the perspective of POI's net power, where the net power is defined as the difference between the power generated from the IBR and consumed by local loads.
- The local load (i.e., the CPL in this case) can absorb active power at the connected bus so that more active power is permitted from the IBR. This is revealed

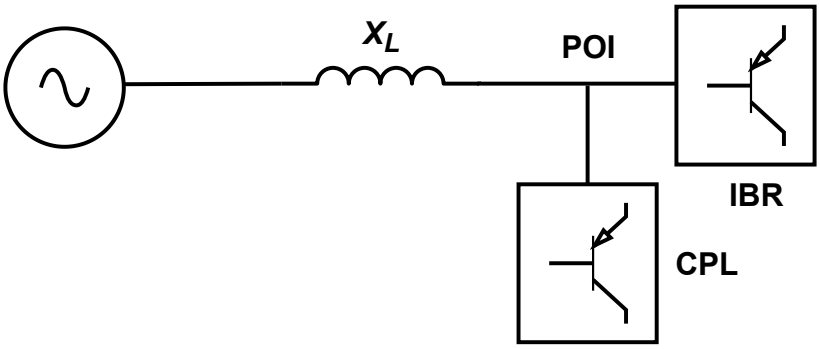

Fig. 16: Single line diagram of the SPIB-CPL system.

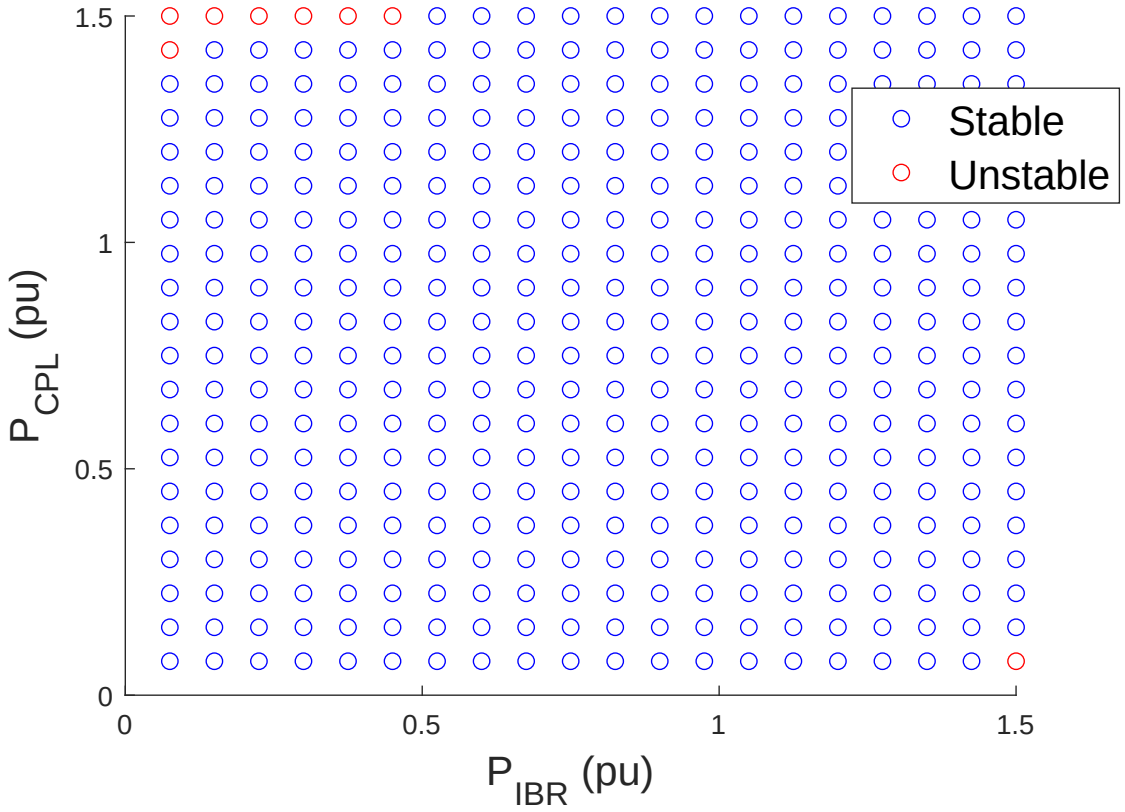

Fig. 17: Stability under different IBR-CPL combinations of the SPIB-CPL system after being disturbed by a fault.

by comparing the bottom row in the figure with the row above. If the CPL absorbs 0.075 p.u. power and IBR outputs 1.5 p.u. power, the system cannot recover from a fault. However, increasing the consumed power of CPL to 0.15 p.u. can facilitate the recovery of the system. From the PMR point of view, the unstable

case yields $PMR = \frac{1.5}{1.5-0.075}$ and $PMR = \frac{1.5}{1.5-0.15}$ for the stable case. Moreover, if examining the diagonal cases, the PMR is approximately infinite since the IBR output matches the consumption of CPL, resulting in the denominator of the PMR being zero. As a result, for the source-load coexisting power systems, a higher PMR implies a stronger grid.

- CPL may degrade the system stability since no terminal AC voltage support is adopted. Comparing the top-left area to the bottom-right area (both areas consists of red dots), it is found that when CPL dominates, the system is prone to lose stability after being disturbed by a fault. From the PMR viewpoint, the CPL is a PQ bus, and the IBR is a PV bus. Based on the analysis in Section 4.2.3, AC voltage control benefits the system strength. When CPL dominates, the connected bus can be viewed as a PQ bus rather than a PV bus.
- PMR is naturally an effective metric for large-signal grid strength of multi-infeed, source-load coexisting power systems.

5 Conclusion

This report summarises the explorations of system strength metrics of the "Strength to Connect" NIA project. The following work has been accomplished:

- The concept of system strength is comprehensively reviewed, and the distinction between small- and large-signal system strength is discussed in WP1.
- A small-signal system strength metric named Impedance Margin Ratio (IMR) is proposed and well-studied in WP1. It is a whole-system assessment that accounts for the dynamics of the apparatus at all nodes, local and remote to the node in question.
- A large-signal system strength metric named Power Margin Ratio (PMR) is proposed in this report. Comprehensive case studies based on electromagnetic transient (EMT) simulations are carried out to illustrate the effectiveness of the PMR and point out its limitations.
- The PMR addresses the problems that existing metrics capture only local interactions between IBRs or simply ignore the contributions of IBRs. The PMR is a power flow-based metric which involves system topology and different control types of IBRs (i.e., GFM, GFL with PV control (GFL_PV), and GFL with PQ control (GFL_PQ)). Based on the characteristics of those control modes, GFM, GFL_PV, and GFL_PQ are modelled as Vθ, PV, and PQ buses, respectively.
- PMR is not a rigorous certificate for transient stability. The actual transient stability is control-dependent, where changes in control parameters of IBR may lead to different stability results. PMR serves as an evaluation tool for large-signal system strength. A larger PMR implies a stronger grid.
- The strong voltage support enhances the post-fault stability of the system. For grid support capability, GFM>GFL_PV>GFL_PQ, which is verified by the PMR.
- Due to the fundamental methodology behind PMR calculation, PMR can naturally adapt to source-load coexisting power systems. Local load can absorb a certain amount of active power, allowing more power to be output from the IBR connected to the same POI.

Several points arise for further investigations:

- The theoretical foundation of the PMR in relation to the dynamical system needs to be fully investigated. The basic idea is to show that a larger PMR implies a greater stability margin or boundary for the system.

- PMR is a quasi-static metric for large-signal system strength. Its calculation relies on the assumption of "static" node types for power flow analysis rather than a detailed mathematical model. The device-level control loops can be included to study the interactions among IBRs in large-signal conditions in a more accurate way.
- It is worth exploring the possibility of a path to bridge the gap between the quasi-static PMR and actual transient stability.

References

[1] F. Blaabjerg, Z. Chen, and S. B. Kjaer, "Power electronics as efficient interface in dispersed power generation systems," *IEEE transactions on power electronics*, vol. 19, no. 5, pp. 1184–1194, 2004.

[2] Y. Gu and T. C. Green, "Power system stability with a high penetration of inverter-based resources," *Proceedings of the IEEE*, vol. 111, no. 7, pp. 832–853, 2022.

[3] C. Henderson, A. Egea-Alvarez, T. Kneuppel, G. Yang, and L. Xu, "Grid strength impedance metric: An alternative to scr for evaluating system strength in converter dominated systems," *IEEE Transactions on Power Delivery*, vol. 39, no. 1, pp. 386–396, 2024. DOI: 10.1109/TPWRD.2022.3233455.

[4] A. Johnson and P. Simango, "Rfg—fast fault current injection," *Nat. Grid ESO*, 2017.

[5] C. Henderson, A. Egea-Alvarez, P. Papadopoulos, *et al.*, "Exploring an impedance-based scr for accurate representation of grid-forming converters," in *2022 IEEE Power & Energy Society General Meeting (PESGM)*, IEEE, 2022, pp. 1–5.

[6] J. Matevosyan, B. Badrzadeh, T. Prevost, *et al.*, "Grid-forming inverters: Are they the key for high renewable penetration?" *IEEE Power and Energy magazine*, vol. 17, no. 6, pp. 89–98, 2019.

[7] Z. Xu, N. Zhang, Z. Zhang, and Y. Huang, "The definition of power grid strength and its calculation methods for power systems with high proportion nonsynchronous-machine sources," *Energies*, vol. 16, no. 4, 2023, ISSN: 1996-1073. DOI: 10.3390/en16041842. [Online]. Available: https://www.mdpi.com/1996-1073/16/4/1842.

[8] B. Badrzadeh *et al.*, "System strength," in vol. 20, CIGRE Science and Engineering, 2021. [Online]. Available: https://e-cigre.org/publication/cse020-cse-020.

[9] Electric Power Research Institute, "Technical reference on the composite load model," EPRI, Technical Report 3002019209, 2020. [Online]. Available: https://www.epri.com/research/products/000000003002019209.